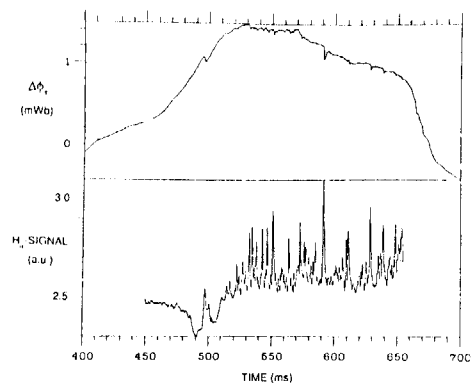

Fig. 1. Diamagnetic loop and Hα signals from the divertor region during neutral beam injection.

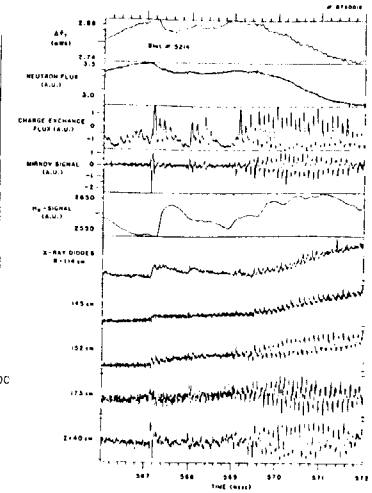

Fig. 2. Signals from various diagnostics during the last part of β-saturation.

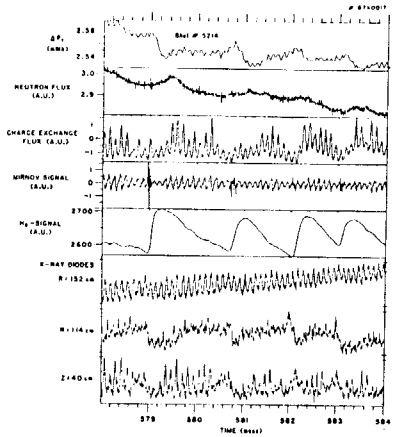

Fig. 3. Signals from different diagnostics during a part of the β-collapse phase.

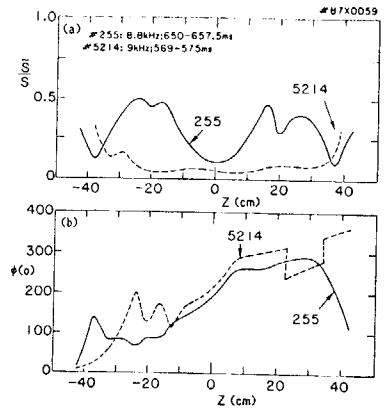

Fig. 4. Comparison of the amplitude modulation and the phase change of the n=1 continuous mode during the β-collapse phase for medium q-edge medium-β (#255), and for high q-edge high β-poloidal (#5214).

BETA LIMITS AND MHD ACTIVITY IN TFTR

A W Morris†, E D Fredrickson, K M McGuire, M G Bell, M S Chance, R J Goldston, R Kaita, J Manickam, S S Medley, N Pomphrey, S D Scott, MC Zarnstorff

Princeton University, Plasma Physics Laboratory, Princeton New Jersey

High power tangential neutral beam injection into TFTR [1] has allowed a study of a variety of MHD phenomena at lower ion collisionality ($\nu_{*i} \sim 10^{-2} - 10^{-3}$) than was possible on smaller tokamaks. The parameter regime for the beta limit studies is 0.5MA< I_p <1.3MA, 5MW< P_{inj} <20MW, 0.5-2.0s injection, R_{geom} = 2.3 – 2.57m (usually 2.45m), a_p = 0.6 – 0.85m (usually 0.8m), 3 < q_{cyl} < 12 with low pre-injection density in a well conditioned vessel. A beta limit exists at high q that is substantially below that expected from simple application of the Troyon limit. Some discussion of phenomena at low q ($q_\psi(a) = 3, 2.5$) will also be given.

Discharges near the β limit: The chief characteristics of the β limit as observed in TFTR are discussed in [2]. Fig 1 shows the envelope of the TFTR data along with the location of some discharges with coherent MHD activity. Although the bound at high q_{cyl} is lower than the Troyon limit [3], q_{cyl} and the profiles are different from those used in that study. Calculations with the PEST code reveal that the plasmas may be unstable to $n = 1$ ideal-MHD modes, with $n = 2$ stable. $q(0) \approx 1 - 1.5$ excludes the broader current profiles required for higher β_n at high $q(a)$. High-n ballooning modes are calculated (in a torus but without FLR corrections) to be unstable over part of the profile in some cases. In general, however, the steepest calculated pressure gradients appear in the shots with best confinement, and this indicates that such modes would affect transport only in the best discharges. Attempts to exceed the TFTR β limit have been made using lower I_p at high P_{inj}. No improvement is found and in fact there is a dependence on I_p: the attainable β_n falls for I_p < 0.7MA ($q_{cyl} \sim 7$). It is also found that there is an optimum P_{inj} for a given I_p, above which the achievable β fails to increase or drops. This optimum is about 11MW for 800kA but has not appeared at 19MW for 1MA.

The β limit is manifest in one of two ways: i) the plasma disrupts either with loss of plasma current, or with loss of typically 50% of the kinetic energy content or ii) the energy content reaches a maximum, then falls with time at constant P_{inj}. For ii), with $I_p \leq$ 1MA, $n_e(r)$ broadens and $T_e, T_i(0)$ and the neutron emission (I_n) fall, almost always accompanied by coherent MHD activity. As I_p is raised, however, a similar collapse of the energy content is sometimes seen, but far from the β limit. This is not always associated with MHD activity, and the discharge may be reverting to TFTR high I_p, n_e confinement scaling, and is at present thought to be a different phenomenon. The presence of MHD activity does not depend just on macroscopic parameters such as $\beta_p, q(a)$ (Fig 1), and the value of $q(0)$ is expected to be important. The target plasma generally has sawteeth ($r_{inv} \sim 5 - 10$cm) which disappear at the start of injection. Experiments with I_p ramped down (typically 1.2MA to 0.9MA in 0.25s, ending just before injection) have produced some high q_{cyl} shots with sawteeth and bursting $m = 1$ modes during NBI with no other MHD activity for 2s injection, consistent with a high current density being frozen into the core. Changes in the injection angle and $P_{co}/P_{counter}$ (and hence in the beam driven currents) have had no reproducible effect on the MHD activity. Possible changes in Z_{eff} and impurities have yet to be investigated.

As reported in [2] perhaps the most remarkable feature of the MHD behaviour of these high-q plasmas is the occurrence of $m = 3, n = 2$ modes in the absence of $n = 1$ activity. Fig 1 shows that (3,2) modes are common and that they appear over a wide range of parameter space (particularly for behaviour (ii) above). (2,1) modes cover a similar range, but $m = 1$ modes and sawteeth are rare at high q (except with current ramp down). $f_{mode} < 20$kHz,50kHz for the (2,1), (3,2) modes respectively. A few good confinement discharges show a centrally localised higher m mode (from SXR array), but this is apparently benign. The (3,2) modes are identified using Mirnov coils at the vessel wall ($R = 2.65$m,$a = 1.10$m, $\Delta\theta = 22.5°$) and are only observed (for high q_{cyl}) with high power auxiliary heating, when pressure and neoclassical effects on MHD theory are expected to be significant. The low value of m at the wall is unambiguous despite the high values of $q(a), \beta_p$. The absence of (3,2) modes in current ramp-down discharges suggests that high $q(0)$ may destabilise this mode (Δ' calculations indicate $q(0) > 1.3$ is unstable) and that $q(0)$ (or $r_{q=1}$ before injection) is indeed an important parameter. The soft x-ray (SXR) signals are consistent with a (3,2) island: there is one more phase change than expected for an ideal-MHD (3,2) distortion. The data indicates a displacement of $\sim 10cm$ at $r = 25cm$ is typical, consistent with estimates of the island size from $\tilde{B}_\theta(wall)$. (2,1) modes of similar size are observed interchangeably with (3,2) modes, and are also apparently resistive - the internal structure is more complex than for the $m = 2$ second harmonic of $m = 1$ sawtooth precursors.

Calculations of I_n give some indication of a loss/redistribution of fast particles during MHD activity. Transport codes (SNAP and TRANSP codes), without beam loss processes, are used. At low I_p(600kA) and $\overline{n_e}$, I_n is over-estimated (typically by a factor 2) for cases with strong MHD activity and I_n falling by 30 – 50% during injection: n_{beam} is too high in the code, suggesting loss of beam ions is required. Time dependent calculations are less sensitive to systematic errors and show the discrepancy appears when I_n begins to fall. At higher I_p, $I_{n,calc}/I_{n,measured}$ does not change as much, but the contribution to $I_{n,calc}$ from beam ions rises and that from thermal ions falls. Estimates of the influence of the low-m, n ripple ($\delta r/R \sim 3\%$ near the island for observed modes) on the trapped thermal and beam ions [4] suggests that their transport could indeed be significantly affected, depending on the velocity profile. A loss/redistribution mechanism for passing ions may also be required to explain the data.

At lower q, or with current ramp down (see above) sawteeth or bursts of $n = 1$ activity appear (Fig 2). The bursts and oscillations are visible in the charge exchange signal only near the injection energy and are most pronounced for near perpendicular views (for $R_{tan} = 0.91$m, 1.47m but not 2.13m). f_{mode} falls through the burst as with fishbones and the mode reported in [5] and its value (5kHz for near balanced injection) is of the same order as the trapped particle precession rate, but some data suggest f_{mode} changes with the net co-injected power. There is no obvious high frequency burst as reported in [5] and E_{dia}, I_n do not drop, indicating the modes are not harmful at present levels. These modes appear as $m = 1$ on the SXR diodes, but as higher m (~ 5, but not a simple structure) on the Mirnov coils. This is the expected behaviour for an ideal-MHD mode and modelling of the SXR emission for PEST $n = 1$ eigenmodes agrees with experiment in the central region of the plasma.

Disruptions: Fig 3 shows a disruption at the β limit. It is seen that I_{SXR}, I_n fall on a $100\mu s$ timescale (after a gamma burst). E_{dia} falls on a timescale of a few ms: the measurement is limited by the vessel time constant (several ms). The limiter temperature rises in $\sim 20\mu s$ [2].

Note the two-stage drop in I_n. There is a rapidly growing oscillatory precursor ($\tau_g \sim 100\mu s$) which has an $m = 1$ structure in the plasma core. The mode structure on the Mirnov coils is not simple - just as with the $m = 1$ bursts above. The timescale of the growth suggests a pressure driven mode, probably with inadequate time for formation of a large island. The PEST code shows that the growth rate of the $n = 1$ internal kink increases rapidly from zero as $q(0)$ drops below unity for these high β_p discharges and the appearance of a $q = 1$ surface is an attractive model for these disruptions. In general disruptions do not follow a period of degraded confinement with (3,2) or (2,1) modes. It is notable that disruptions can occur far from the β limit [2], early during injection when the beam pressure dominates. Disruptions of the ohmic target plasma at these q values do not occur.

Low-q_ψ operation: Experiments with co-injection and q_ψ close to the rational values 3.0, 2.5 reveal increases of $\sim 15\%$ in E_{dia} and $\sim 50\%$ in particle density after a clear transition, reminiscent of limiter discharges on JFT-2M [6]. There is a drop in toroidal rotation velocity (and hence a temporary energy source from rotational energy and a consequent improvement in heating efficiency [7]) and a sharp fall in the measured H_α emission from the inboard side. There is evidence from SXR and Mirnov signals of a slowly rotating mode (3,1 for $q_\psi = 3$, 5,2 for $q_\psi = 2.5$) at the plasma edge during the transition, correlated with a rotating structure in the H_α emission, which peaks at the x-point of the locking/unlocking mode. This structure is also apparent on the electron temperature (ECE) and suggests that a form of helical divertor may be present. The central plasma continues to rotate, albeit at a reduced speed, as shown by Doppler shift measurements and the simultaneous presence of $n = 1$ modes in the centre of the plasma with a higher frequency than the edge mode.

Conclusions: The β limit as seen on TFTR is close to the limit due to $n = 1$ ideal-MHD modes even in this high q regime. This limit is substantially below the extrapolated Troyon limit. The modes correlated with the degraded confinement appear to be resistive in origin, and appear (experimentally) to be sensitive to $q(0)$ and $q(r)$ near the axis. There is initial evidence that these instabilities play a significant role in the fast ion dynamics. Although the profiles may be close to the high n ideal-MHD ballooning threshold, no direct evidence of ballooning modes has been found. Experiments in limiter discharges with q_ψ near to 3, 2.5 show a transition to a state of apparently improved particle confinement with indications of a stationary helical perturbation.

The authors are grateful for discussions with J Strachan and H Mynick. This work was supported by US DOE contract No DE-AC02-76-CHO-3073.

† Balliol College, University of Oxford, UK.

References:

[1] Strachan, J D *et al* Phys Rev Lett **58**, 1004 (1987)
[2] McGuire, K M *et al*. Proc 11th IAEA Conf, Kyoto, paper A-VII-4 (1986)
[3] Troyon, F, Gruber, R *et al* Plasma Phys and Nucl Fus **26**, 209 (1984)
[4] Mynick, H. Nuclear Fusion **26**, 491 (1986)
[5] Heidbrink, W W *et al* Phys Rev Lett. **57**, 835 (1986)
[6] Odajima, K *et al* Proc 11th IAEA Conf, Kyoto, paper A-III-2 (1986)
[7] Goldston, R J *et al* Proc 11th IAEA Conf, Kyoto, paper A-II-1 (1986)

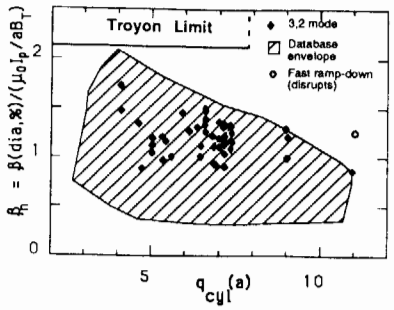

Figure 1: Location of $m = 3, n = 2$ modes and the β limit on TFTR. $q_{cyl} \equiv \frac{5a_p^2 B_\phi}{R_{geom} I_p(MA)}$. The full data set is hatched.

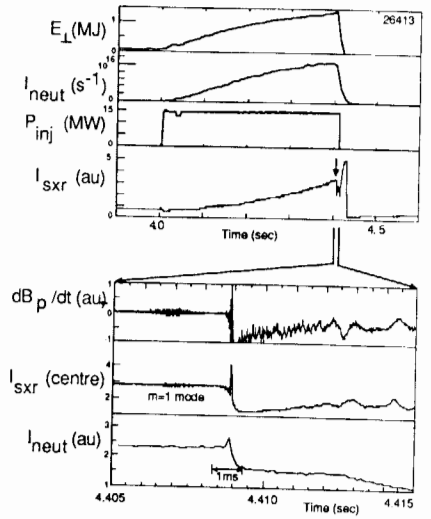

Figure 3: Waveforms for a disruption at the β limit. $I_p = 950kA, P_{inj} = 14.6MW$, $P_{cntr} = 5.6MW, \beta_p = 2.0, \overline{n_e} = 2.9\times10^{19}m^{-3}$, $q_{cyl} = 7.2$. Note I_n falls by $\sim 30\%$ in $100\mu s$. The plasma position changes at 4.409s and I_p decays 4.42-4.44s ($4.5 \times 10^7 A/s$).

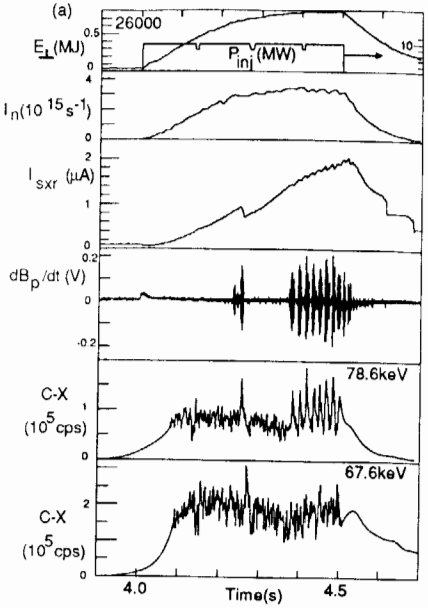

Figure 2: Example of $n = 1$ bursting mode (with a sawtooth at $t = 4.25s$). $P_{co} = P_{counter}$, $I_p = 0.9$MA, $q_{cyl} = 4.1$, $\beta_p = 1.2$. Note absence of effect of the mode on I_n, E_{dia}. In (a) the C-X sampling rate changes at 4.08 and 4.5s. In (b) (not the same shot) the timing of the C-X data is uncertain to a few ms and is from 4.33-4.34s only.

TEMPERATURE SCALING OF OHMICALLY HEATED DEUTERIUM PLASMAS IN TEXTOR

H. Kever, G. Waidmann

Institut für Plasmaphysik der Kernforschungsanlage Jülich GmbH,
Association EURATOM-KFA, 5170 Jülich 1, FRG

Introduction.
Measurements of the electron temperature and the energy content by two independent methods, i.e. ECE - measurement of T_e and measurement of the plasma diamagnetism to obtain β_{pol}, have been performed on TEXTOR to include larger plasma currents and higher toroidal magnetic field strengths. The results of both measurements confirm scaling laws derived from the assumption of anomalous electron heat conduction in an Ohmically heated plasma with Spitzer resistivity. Dependences of the electron temperature on the plasma density n are attributed to systematic changes in Z_{eff} which enters through the resistance. The possibility to achieve thermonuclear burn in larger devices by increasing the plasma currents is discussed.

Electron temperatures from ECE-measurements.
The diagnostic technique has been described elsewhere /1/. In the plasma core, the temperature is determined by the input of Ohmic heating power and the losses due to thermal conduction; radiation losses for not too high degrees of plasma contamination are small. Therefore, in the steady state (and for the temporal averages if oscillatory contributions enter the quantities in question) the power balance per unit length for a plasma with cross-section of radius r reads

$$\pi r^2 n_j^2 - 2\pi r Q_r = 0 \quad , \qquad (1)$$

where near the axis $n_j^2 \approx n_{0j}^2 = \text{const}$ (index 0 denotes the axis), and Q_r is the radial energy flux density. If for the latter

$$Q_r = -K_e \frac{\partial T}{\partial r}$$

i.e. neglecting convective contributions, then upon integration of equ. (1) up to a radius $r_1 \ll a$ with $K_e \approx$ const, we obtain

$$r_1^2 n_j^2 = 2 K_e [T(r=0) - T(r_1)].$$

For temperatures distributed (in the temporal average) according to $T = T_0[1-(r/a)^2]^\lambda$, the difference between the temperatures at the center of the plasma and at $r = r_1$ becomes

$$T_0 - T(r_1) \approx \lambda r_1^2 T_0/a^2.$$

Writing the expression for the Spitzer resistivity $\eta = \gamma(Z_{eff}) Z_{eff} \eta_1/T^{3/2}$, where η_1 is the value of the plasma resistivity for $Z_{eff}=1$ and $T_0 = 1$ keV, and $\gamma(Z_{eff})$ is the correction factor of the resistivity for $Z_{eff} \neq 1$ (compared to the Lorentz gas approximation), then the power balance becomes